arXiv:1411.1210v1 [quant-ph] 5 Nov 2014

Dynamics of genuine multipartite entanglement under local non-Markovian dephasing

Mazhar Ali

Department of Electrical Engineering, COMSATS Institute of Information Technology, 22060 Abbottabad, Pakistan

Abstract

We study dynamics of genuine entanglement for quantum states of three and four qubits under non-Markovian dephasing. Using a computable entanglement monotone for multipartite systems, we find that GHZ state is quite resilient state whereas the W state is the most fragile. We compare dynamics of chosen quantum states with dynamics of random pure states and weighted graph states.

Keywords: Genuine entanglement, non-Markovian, random states
PACS: 03.65.Yz, 03.65.Ud, 03.67.Mn

1. Introduction

Quantum entanglement not only defies our classical intuition but also finds its role in several practical applications devised to harness the power of quantum physics. The technological promise of entanglement has attracted lot of interest to develop a theory of its own, which deals with its characterization and quantification, optimal detection in theory and experiments, and the methods to reverse the inevitable process of decoherence [1, 2]. As entangled states are desired to generate and manipulate in experiments, therefore it is essential to study the effects of various environments on entanglement. In recent years, this study has received considerable attention and is currently an active area of research [3]. The dynamics of entanglement under various environments were studied for both bipartite and multipartite systems [4, 5, 6, 7, 8, 9, 10, 11, 12, 13, 14]. Several works of entanglement dynamics considered bipartite aspects of entanglement of multipartite states [8], however this can only give partial results because entanglement in multipartite systems is different than the entanglement among different partitions. As theory of multipartite entanglement is still in progress, one can make statements on lower bounds of entanglement but not on its exact value [9]. The exact value of multipartite entanglement was only calculated for specific model of decoherence and specific quantum states [11]. In addition, in order to comment on the robustness or fragility of a state, one need to compare its dynamics with dynamics of random states. Recently, we have addressed these issues and studied the robustness of several multipartite

states by investigating an exact measure of genuine multipartite entanglement under Markovian environments [15].

In this work, we extend our study to dynamics of genuine entanglement under a specific type of non-Markovian noise. Although, the approximation of weak interaction and no back action of environment on principal system might be valid for certain circumstances, however in reality most systems are non-Markovian. It is important to simulate the effects of non-Markovian environments on genuine entanglement. Recent progress in the theory of multipartite entanglement has enabled us to study decoherence effects on actual multipartite entanglement and not on entanglement among bipartitions. In particular, the ability to compute genuine negativity for multipartite systems has eased this task [16]. We find that under non-Markovian dephasing, GHZ state appears to be resilient as it repeats the collapse and revival of genuine entanglement for long time. On the other hand, the W state turns out to be most fragile state. All other quantum states of four qubits exhibit behavior between these two extremes. We compare the dynamics of chosen quantum states of three and four qubits with dynamics of random pure states and weighted graph states.

This paper is organized as follows. In section 2, we briefly discuss our model of interest. We review the concept of entanglement for multipartite systems in section 3 where we also describe the method to compute genuine negativity and discuss the quantum states which we study in this work. In section 4, we provide results and finally we conclude our work in section 5.

2. Local non-Markovian dephasing model

The model which we intend to study here is well known [17]. Recently, this model has also been studied for sudden change in dynamics of quantum discord [18]. We consider a dephasing with colored noise with dynamics described by a master equation [17, 18]

$$\dot{\rho}(t) = \mathcal{K}\,\mathcal{L}\,\rho\,, \tag{1}$$

where $\mathcal{K}$ is time-dependent integral operator whose action on a function is defined as

$$\mathcal{K}\phi = \int_0^t dt'\, k(t-t')\phi(t')\,, \tag{2}$$

with $k(t-t')$ is a kernel which determines the type of environment memory. ρ is density matrix of the principal system and $\mathcal{L}$ is the Lindblad super-operator which describes dynamics of principal system as a result of interaction with environment. Note that in the absence of $\mathcal{K}$ in Eq.(1) one usually get the master equation with Markovian approximation. For a concrete example of a system, we may consider the time-dependent Hamiltonian [17, 18]

$$H(t) = \hbar \sum_{i=1}^{3} \Gamma_i(t)\,\sigma_i\,, \tag{3}$$

where σ_i are the Pauli matrices and $\Gamma_i(t)$ are the independent random variables which obey statistics of a random telegraph signal defined as $\Gamma_i(t) = a_i\,(-1)^{n_i(t)}$. The random variable $n_i(t)$ has a Poisson distribution with a mean $t/(2\,\tau_i)$ and a_i is an independent random variable taking values $\pm a_i$. This model applies to any two-level quantum system interacting with an environment having random telegraph signal noise. As an example, this could describe a two-level atom subjected to a fluctuating laser field that has jump type random phase noise [17].

Using von Neumann equation of motion $\dot{\rho} = -(\mathrm{i}/\hbar)[H,\,\rho]$, we can write the solution for density matrix of two level system as

$$\rho(t) = \rho(0) - \mathrm{i}\int_0^t dk \sum_i \Gamma_i(k)[\sigma_i,\,\rho(k)]\,. \tag{4}$$

Substituting this equation back into von Neumann equation and performing stochastic average, we obtain [17]

$$\dot{\rho}(t) = -\int_0^t dt' \sum_k e^{-(\frac{t-t'}{\tau_k})} a_k^2\,\left[\sigma_k,\,[\sigma_k,\,\rho(t')]\right], \tag{5}$$

where the correlation functions of random telegraph signal

$$\langle \Gamma_j(t)\Gamma_k(t')\rangle = a_k^2\, e^{-\frac{|t-t'|}{\tau_k}}\,\delta_{jk} \tag{6}$$

have been inserted. It turns out that the dynamical evolution generated by Eq.(5) is completely positive when two of the a_k are zero. This would correspond to a physical situation where noise only acts in one direction. In particular if $a_1 = a_2 = 0$, and $a_3 = a$, then the dynamics of the system is that of a dephasing with colored noise. The Kraus operators describing the dynamics of two-level system are given as [17, 18]

$$\begin{aligned} K_1 &= \sqrt{[1+\Lambda(\nu)]/2}\,I_2 \\ K_2 &= \sqrt{[1-\Lambda(\nu)]/2}\,\sigma_3\,, \end{aligned} \tag{7}$$

where I_2 is 2×2 identity matrix and $\Lambda(\nu) = e^{-\nu}\left[\cos(\mu\nu) + \sin(\mu\nu)/\mu\right]$, with $\mu = \sqrt{(4a\tau)^2 - 1}$ and $\nu = t/(2\tau)$ is the dimensionless time. The Kraus operators satisfy the normalization condition $\sum_i\, K_i^\dagger(t)\,K_i(t) = I$.

As we are interested in three and four qubit systems, the time evolution of an initial density matrix can be written as

$$\rho(t) = \sum_i\, M_i(t)\,\rho(0)\,M_i^\dagger(t), \tag{8}$$

where $M_i(t)$ are the Kraus operators, satisfying the normalization condition $\sum_i\, M_i^\dagger(t)\,M_i(t) = I$. For three qubits, there are 8 such operators, that is, $M_1 =$

$K_1^A K_1^B K_1^C$, $M_2 = K_1^A K_1^B K_2^C$,..., $M_8 = K_2^A K_2^B K_2^C$. We have omitted the tensor product symbol between these operators. Similarly, the respective 16 operators for four qubits are $M_1 = K_1^A K_1^B K_1^C K_1^D$, $M_2 = K_1^A K_1^B K_1^C K_2^D$,...,$M_{16} = K_2^A K_2^B K_2^C K_2^D$.

The time evolved density matrix for a single qubit can directly be computed and it is given as

$$\rho(t) = \begin{pmatrix} \rho_{11} & \gamma\rho_{12} \\ \gamma\rho_{21} & \rho_{22} \end{pmatrix}, \tag{9}$$

where

$$\gamma = \mu^{-1}\, e^{-\nu}[\,\sin(\mu\nu) + \mu\,\cos(\mu\nu)\,]. \tag{10}$$

For more qubits, the calculation of density matrices is straightforward.

3. Multipartite entanglement and quantum states

In this section, we briefly review the concept of entanglement in multipartite systems and discuss the particular quantum states which we study in this article. We want to emphasize at this stage that material in this section is already known in the literature and we cite them appropriately.

3.1. Genuine multipartite entanglement and multipartite negativity

We review genuine multipartite entanglement by considering three particles A, B, and C, as the generalization to more parties is straightforward. A state is called separable with respect to some bipartition, say, $A|BC$, if it is a mixture of product states with respect to this partition, that is, $\rho^{sep}_{A|BC} = \sum_j\, q_j\, |\phi^j_A\rangle\langle\phi^j_A| \otimes |\phi^j_{BC}\rangle\langle\phi^j_{BC}|$, where $q_j \geq 0$ and $\sum_j q_j = 1$. Similarly, separable states for the two other bipartitions are $\rho^{sep}_{B|AC}$ and $\rho^{sep}_{C|AB}$. A state is called biseparable if it can be written as a mixture of states which are separable with respect to different bipartitions, that is

$$\rho^{bs} = p_1\, \rho^{sep}_{A|BC} + p_2\, \rho^{sep}_{B|AC} + p_3\, \rho^{sep}_{C|AB}\,. \tag{11}$$

A state is genuinely multipartite entangled if it is not biseparable. In this paper, we study dynamics of this genuine multipartite entanglement.

Recently, it has been worked out to detect and characterize multipartite entanglement by using positive partial transpose mixtures (PPT mixtures) [16]. We recall that a two-party state $\rho = \sum_{ijkl}\, \rho_{ij,kl}\, |i\rangle\langle j| \otimes |k\rangle\langle l|$ is PPT if its partially transposed matrix $\rho^{T_A} = \sum_{ijkl}\, \rho_{ji,kl}\, |i\rangle\langle j| \otimes |k\rangle\langle l|$ has no negative eigenvalues. It is known that separable states are always PPT [19]. The set of separable states with respect to some partition is therefore contained in a larger set of states which has a positive partial transpose for that bipartition.

The states which are PPT with respect to fixed bipartition may be called $\rho^{PPT}_{A|BC}$, $\rho^{PPT}_{B|AC}$, and $\rho^{PPT}_{C|AB}$. We ask whether a state can be written as

$$\rho^{PPTmix} = p_1\, \rho^{PPT}_{A|BC} + p_2\, \rho^{PPT}_{B|AC} + p_3\, \rho^{PPT}_{C|AB}\,. \tag{12}$$

Such a mixing of PPT states is called a PPT mixture. The genuine multipartite entanglement of four or more particles can be detected and quantified in an analogous manner by considering all bipartitions (like one party vs. $N-1$ parties, two parties vs. $N-2$ parties, etc.).

As any biseparable state is a PPT mixture, therefore any state which is not a PPT mixture is guaranteed to be genuinely multipartite entangled. The prime advantage of considering PPT mixtures instead of biseparable states is that PPT mixtures can be fully characterized with the method of semidefinite programming (SDP) [20]. In general, the set of PPT mixtures is a very good approximation to the set of biseparable states and delivers the best known separability criteria for many cases, nevertheless there are multipartite entangled states which are PPT mixtures [16]. It is also interesting to note that there are biseparable states which may have negative partial transpose (NPT) under each partition [2].

It has been shown [16] that a state is a PPT mixture iff the following optimization problem

$$\min \mathrm{Tr}(\mathcal{W}\rho) \tag{13}$$

under the constraint that for all bipartitions $M|\bar{M}$

$$\mathcal{W} = P_M + Q_M^{T_M}, \quad \text{with } 0 \leq P_M \leq I \text{ and } 0 \leq Q_M \leq I \tag{14}$$

has a positive solution. The constraints reflect that $\mathcal{W}$ is a decomposable entanglement witness for any bipartition. If this minimum is negative then ρ is not a PPT mixture and hence genuinely multipartite entangled. Since this is a semidefinite program, the minimum can be efficiently computed and the optimality of the solution can be certified [20]. We use the programs YALMIP and SDPT3 [21] to solve SDP. We also use implementation which is freely available [22].

This approach can be used to quantify genuine entanglement as the absolute value of the minimization was shown to be an entanglement monotone for genuine multipartite entanglement [16]. In the following, we will denote this measure by $E(\rho)$. For bipartite systems, this monotone is equivalent to *negativity* [23]. For a system of qubits, this measure is bounded by $E(\rho) \leq 1/2$ [24].

3.2. Multipartite entangled states

We are interested in several families of states in this work. Two important families of states, namely the GHZ states and the W states for N qubits are given as

$$\begin{aligned} |GHZ_N\rangle &= \frac{1}{\sqrt{2}}(|00...0\rangle + |11...1\rangle), \\ |W_N\rangle &= \frac{1}{\sqrt{N}}(|00...001\rangle + |00...010\rangle + \ldots + |10...000\rangle). \end{aligned} \tag{15}$$

GHZ state has always maximum value of monotone, that is, $E(|GHZ_N\rangle\langle GHZ_N|) = 1/2$, whereas for the W state, numerical value depends on the number of qubits. For three qubits $E(|W_3\rangle\langle W_3|) \approx 0.443$ and for four qubits $E(|W_4\rangle\langle W_4|) \approx 0.366$.

Several interesting states for four qubits are Dicke state $|D_{2,4}\rangle$, the singlet state $|\Psi_{S,4}\rangle$, the cluster state $|CL\rangle$ and the so-called χ-state $|\chi_4\rangle$, given as

$$\begin{aligned}
|D_{2,4}\rangle &= \frac{1}{\sqrt{6}}[|0011\rangle + |1100\rangle + |0101\rangle + |0110\rangle + |1001\rangle + |1010\rangle]\,, \\
|\Psi_{S,4}\rangle &= \frac{1}{\sqrt{3}}[|0011\rangle + |1100\rangle - \frac{1}{2}(\,|0101\rangle + |0110\rangle + |1001\rangle + |1010\rangle)]\,, \\
|CL\rangle &= \frac{1}{2}[|0000\rangle + |0011\rangle + |1100\rangle - |1111\rangle], \\
|\chi_4\rangle &= \frac{1}{\sqrt{6}}[\sqrt{2}|1111\rangle + |0001\rangle + |0010\rangle + |0100\rangle + |1000\rangle], \qquad (16)
\end{aligned}$$

respectively. All these states are maximally entangled with respect to multipartite negativity, $E(|D_{2,4}\rangle\langle D_{2,4}|) = E(|\Psi_{S,4}\rangle\langle\Psi_{S,4}|) = E(|CL\rangle\langle CL|) = E(|\chi_4\rangle\langle\chi_4|) = 1/2$. These states along with their properties are discussed in Ref. [2].

3.3. Random pure states

We describe the generation of random pure states. A state vector randomly distributed according to the Haar measure can be generated as follows [25]: First, we generate a vector such that both the real and the imaginary parts of the vector elements are Gaussian distributed random numbers with a zero mean and unit variance. Second we normalize the vector. It is easy to prove that the random vectors obtained this way are equally distributed on the unit sphere [25]. We stress that we generate random pure states in the global Hilbert space of three- and four qubits, so the unit sphere is not the Bloch ball.

3.4. Weighted graph states

Another important family of multi-qubit states are weighted graph states which also includes states such as GHZ and cluster states [26, 27]. These states have been studied for entanglement properties of spin gases [26].

We consider a graph as a set of vertices and edges, where the vertices may denote the physical systems (qubits) and the edges represent the interactions among physical systems. We initially prepare all the qubits in the state $|+\rangle = (|0\rangle + |1\rangle)/\sqrt{2}$. For any pair of qubits k, l which are connected with an edge, we apply an interaction via Hamiltonian

$$H_{kl} = \frac{1}{4}\,(I - \sigma_z^{(k)}) \otimes (I - \sigma_z^{(l)})\,. \qquad (17)$$

The resulting unitary transformation is $U_{kl} = \mathrm{e}^{i\,\phi_{kl}\,H_{kl}}$, where ϕ_{kl} is the interaction time. The generated state after this process is called the weighted graph state given as

$$|WGS\rangle = \bigotimes_{k,l} U_{kl}(\phi_{kl})\,|+\rangle^{\otimes N}\,. \qquad (18)$$

The weighted graph state is uniquely determined by the $N(N-1)/2$ parameters ϕ_{kl}, which form only a small subset of all pure states described by $2^N - 1$ parameters. However, many interesting belong to this class. We have chosen the interaction times $\phi_{kl} \in [0, 2\pi]$ uniformly distributed in the interval to generate these states. For the choice $\phi_{kl} = \pi$ or $\phi_{kl} = 0$, the usual graph states (also containing the GHZ and cluster states) appear. We note that the temporal order of the interaction does not matter because the unitaries U_{kl} commute. Some generalizations of these states have been investigated recently [28].

We point out here that all random states generated by these two techniques are genuinely entangled. As described above, the weighted graph states may include GHZ states and cluster states, however this does not mean that every random state generated is equivalent to only these two types of states. Therefore, it is meaningful to compare the dynamics of specific states with dynamics of random states [15].

4. Results

In this section, we present our results for quantum states discussed in previous section. First we discuss the effect of non-Markovian dephasing on genuine entanglement of three qubits.

Figure 1 shows the multipartite negativity $E(\rho)$ plotted against the dimensionless time $\nu = t/(2\tau)$. We have chosen $a = 1s$ and $\tau = 5s$ which are for non-Markovian region [18]. The solid line denotes the GHZ state whereas dotted line is for the W state. It can be seen that the genuine entanglement of GHZ state first goes to zero and then revives again with a lower peak than the previous one. This collapse and revival of genuine entanglement for GHZ state repeats itself for sufficiently long time, however each time with a lower peak than the earlier ones. This suggest that GHZ state is resilient state against non-Markovian dephasing. This observation is similar to our recent studies where we have observed that GHZ state is quite robust under Markovian dephasing [15]. We stress that in our previous study [15], we have used logarithmic derivative of genuine entanglement to claim the robustness of GHZ state under Markovian dephasing, whereas here we use the term "resilience" to this several time repetition of collapse and revival of genuine entanglement for GHZ state. Several authors have studied the robustness of entanglement [29, 30]. In [29], the authors have identified most robust states under local decoherence used the definition introduced before [8], whereas, the authors of Ref.[30] considered asymptotic long-time dynamics of initial states and identified two different classes of states, one class is fragile even there remains some coherence in the system and the second class as most robust states which become disentangled only when decoherence is perfect. However, as described above, our approach is different than these studies.

In contrast, the W state is very fragile under non-Markovian dephasing. The collapse and revival of genuine entanglement for W state disappear earlier. The revival of genuine entanglement for the W state also takes a little longer time than the GHZ state. This observation is similar to Markovian dephasing where

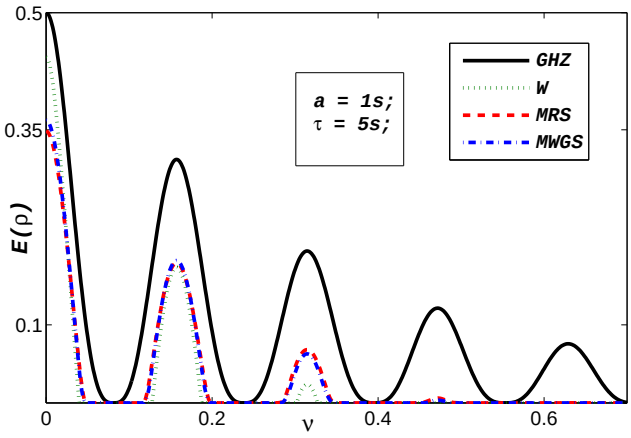

Figure 1: Multipartite negativity for various three-qubit states is plotted against parameter ν. We observe different rates of collapse and revival of genuine entanglement for different states. GHZ state is resilient state whereas W state is fragile.

the W state is found to be quite fragile [15]. In addition, we plot the mean values of genuine negativity for random pure states (MRS) denoted by dashed line and weighted graph states (MWGS) denoted by dashed-dotted line for comparison purpose. It is interesting to note that genuine entanglement behavior of both type of random states almost resemble to the W state. At this stage, we want to remind the readers that our method to detect the genuine entanglement is not always perfect. If this measure is positive then the state is guaranteed to be genuinely entangled, however, if it is zero, then in general, we do not know whether the state is entangled or not. Except for the GHZ state which we discuss below in detail, we can not say with certainty that all zero values of genuine negativity in Figure 1 and all subsequent figures correspond to states with no entanglement of any type.

An interesting property of the dynamical process is the fact that all zero elements of the initial density matrix remain zero. For GHZ state the only non-zero density matrix elements are ρ_{11}, $\rho_{18}(t)$, $\rho_{81}(t)$ and ρ_{88}. A recent result on the detection of genuine entanglement states that for biseparable states, the inequality

$$|\rho_{18}| \leq \sqrt{\rho_{22}\rho_{77}} + \sqrt{\rho_{33}\rho_{66}} + \sqrt{\rho_{44}\rho_{55}} \tag{19}$$

is satisfied and the violation implies genuine entanglement [31]. This criterion is a necessary and sufficient condition for GHZ-diagonal states [31]. We will not go into details of GHZ-diagonal states here but for our purpose this criterion would imply that time evolved GHZ state is genuinely entangled if and only if $|\rho_{18}(t)| > 0$, that is,

$$|\gamma^3/2| > 0, \quad \Longrightarrow f(\nu) = |\sin(\mu\nu) + \mu\cos(\mu\nu)| > 0\,, \tag{20}$$

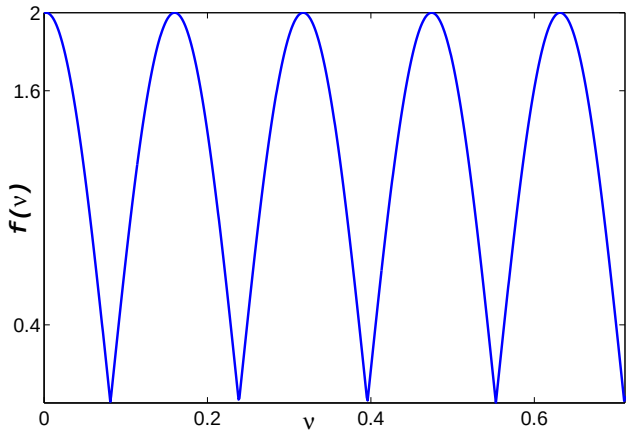

Figure 2: Absolute value of function $f(\nu)$ scaled down to a factor of 10, is plotted against parameter ν.

where γ is defined in Eq.(10). In Figure 2, we plot the function $f(\nu)$ scaled down to a factor of 10 against parameter ν with $\mu = \sqrt{399}$ for chosen values of a and τ. A close comparison of Figure 2 with Figure 1 reveals that for those points where $f(\nu)$ is zero, the genuine entanglement for GHZ state is also zero and vice versa. Actually, at these points the off-diagonal elements of any arbitrary time-evolved density matrix disappear completely, so entanglement of any type disappear as well. This fact is evident in Figure 1. It also explains the collapse and revivals of genuine entanglement of GHZ state at these instances. It was shown [32] that phase-damping channels are called locally entanglement-annihilating if and only if the off-diagonal elements disappear completely. This happens only at times when $f(\nu) = 0$. Therefore, only at these points, being entanglement-annihilating coincides with being entanglement-breaking. It is interesting to note that disappearance of genuine entanglement only coincides with these instances for GHZ state. For other states, there are intervals where off-diagonal elements are not zero but our criterion fails to detect whether there is entanglement of any type as discussed before.

The presence of exponential factor in the definition of γ also explains the gradually decaying peaks of genuine entanglement of all initial states. As every off-diagonal element of the time-evolved density matrix is being multiplied by a factor γ^r with $r = 1$, 2, or 3, therefore as $f(\nu)$ is zero necessarily means γ is zero and γ is maximum when $f(\nu)$ is maximum. This is the reason that all states have their peak value of genuine entanglement at instances when $f(\nu)$ is maximum. This feature is also evident from Figures 4 and 5.

As the behavior of GHZ state is very different than all other states, therefore in order to get some more insight, we explore the effects of decreasing the degree of non-Markovianity on its dynamics. By fixing $a = 1s$, the parameter $\tau = 5$

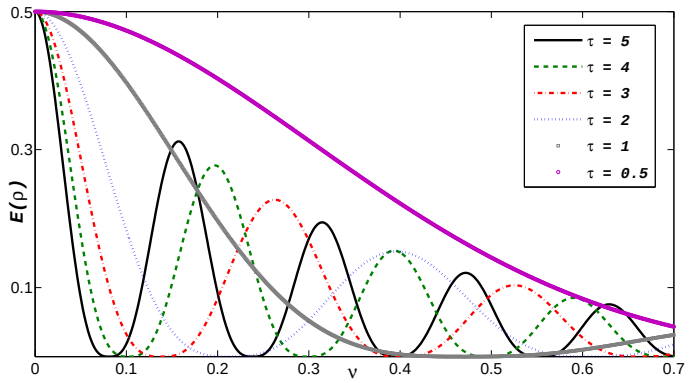

Figure 3: Genuine entanglement for three-qubit GHZ state is plotted against parameter ν. We observe that by decreasing degree of non-Markovianity, collapse and revival of genuine entanglement are also decreased and for $\tau = 0.5$, which corresponds to Markovian case, there are no collapse and revivals.

denotes the non-Markovian case, whereas $\tau = 0.5$ corresponds to Markovian case. Figure 3 shows genuine entanglement of GHZ state for various values of parameter τ plotted against parameter ν. It can be observed that as we decrease the degree of non-Markovianity, the collapses and revivals of genuine entanglement are also decreased and delayed. Finally, for $\tau = 0.5$, there are no collapse and revival of genuine entanglement, as we expect from Markovian dynamics. As we discussed above, for GHZ state to be genuinely entangled, $|\rho_{18}(t)| > 0$, and this value could only be non-zero if γ defined in Eq.(10) is non-zero. As γ depends on μ, which in turn depends on τ, that is, for $\tau = 5$, $\mu = \sqrt{399}$ (non-Markovian case), for such a large value of μ, the sine and cosine functions are considerable and can not be ignored. Hence these functions are responsible for collapses and revivals. On the other hand, for $\tau = 0.5$, we have $\mu = \sqrt{3}$ (Markovian case), which is much smaller than the previous case. So for such a small argument, we can apply small angle approximation to sine and cosine functions. Hence we can explain the corresponding disappearance of collapses and revivals of genuine entanglement for Markovian case.

Figure 4 shows multipartite negativity for 100 random pure states plotted against ν. We also plot mean values of random pure states (MRS) denoted by dashed line and weighted graph states (MWGS) denoted by dashed-dotted line, however they almost overlap and may not be clearly visible.

In Figure 5, we plot multipartite negativity for 100 weighted graph states along with mean values of genuine entanglement for random pure states (MRS) and weighted graph states (MWGS).

Let us now discuss the results for four qubits case. In Figure 6, we plot genuine negativity for various states discussed in previous section. As for the case of three qubits the GHZ state is resilient state whereas the W state is quite

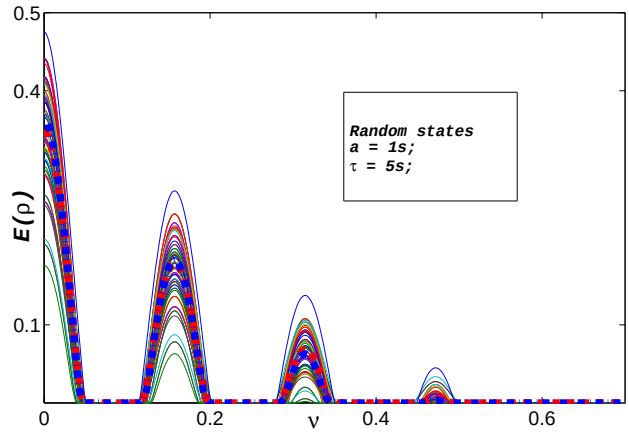

Figure 4: Genuine entanglement for three-qubit random states with mean values of random states and weighted graph states plotted against parameter ν.

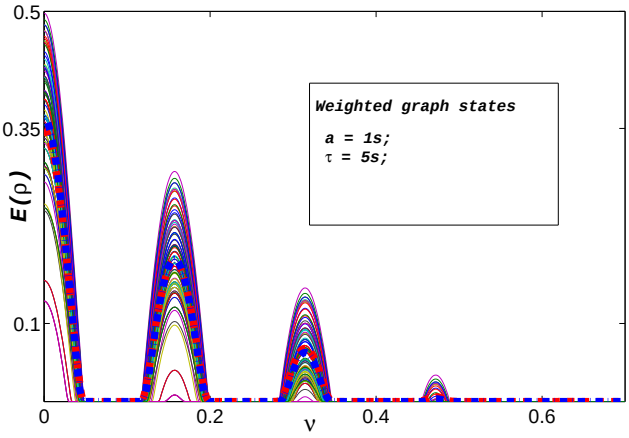

Figure 5: Genuine entanglement for three-qubit weighted graph states with mean values of random states and weighted graph states plotted against parameter ν.

fragile. All other states including random pure states and weighted graph states exhibit a trend in between these two extremes as evident from the Figure 6. As results for the four qubits are almost identical to the three qubits case, therefore we preferred to plot only mean value of genuine entanglement for random states only.

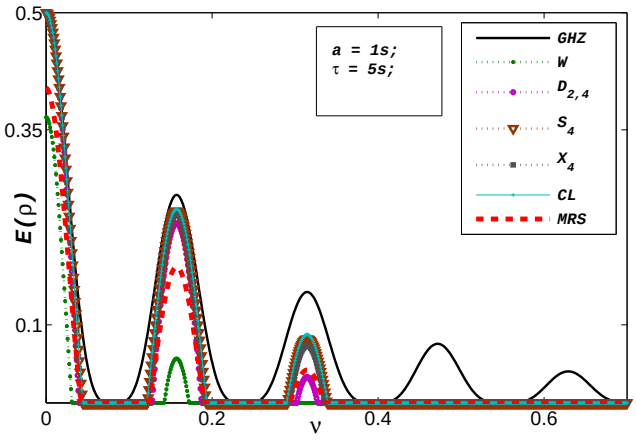

Figure 6: Genuine entanglement for various four-qubit states with mean value of random pure states is plotted against parameter ν.

5. Conclusion

We have studied the behavior of genuine multipartite entanglement under non-Markovian dephasing. Using a computable entanglement monotone for multipartite quantum systems, we have observed the collapses and revivals of genuine entanglement for various quantum states of three and four qubits. We have found that GHZ state is resilient state as it repeats its revival for long time whereas all other states loose their revivals much earlier. We have examined and explained this different behavior of GHZ state. We have found that the W state is the most fragile state similar to Markovian environments. We have compared dynamics of chosen quantum states with dynamics of random pure states and weighted graph states so that we can make meaningful statements about their behavior under decoherence. We found that all random states and weighted graph states show a similar trend as the W state. We stress here that our conclusions are based on a criterion whose positive value for a given quantum state is guaranteed to be genuinely entangled, however, for states which are not detected by this criterion, we are not certain about their entanglement properties. For GHZ state under current dynamics, this criterion provides a necessary and sufficient criterion to detect genuine entanglement.

Acknowledgements

The author is grateful to both anonymous referees for their constructive comments, which brought much clarity and a new Figure 3 in the manuscript.

References

References

[1] R. Horodecki *et al.*, Rev. Mod. Phys. **81**, 865 (2009).

[2] O. Gühne and G. Tóth, Phys. Rep. **474**, 1 (2009).

[3] L. Aolita, F. de Melo, and L. Davidovich, arXiv:1402.3717 [quant-ph]

[4] T. Yu and J. H. Eberly, Phys. Rev. B **66**, 193306 (2002); T. Yu and J. H. Eberly, Phys. Rev. B **68**, 165322 (2003); T. Yu and J. H. Eberly, Phys. Rev. Lett. **93**, 140404 (2004); J. H. Eberly and T. Yu, Science **316**, 555 (2007).

[5] W. Dür and H.J. Briegel, Phys. Rev. Lett. **92**, 180403 (2004); M. Hein, W. Dür, and H.-J. Briegel, Phys. Rev. A **71**, 032350 (2005).

[6] L. Aolita *et al.*, Phys. Rev. Lett. **100**, 080501 (2008).

[7] C. Simon and J. Kempe, Phys. Rev. A **65**, 052327 (2002); A. Borras *et al.*, Phys. Rev. A **79**, 022108 (2009); D. Cavalcanti *et al.*, Phys. Rev. Lett. **103**, 030502 (2009).

[8] S. Bandyopadhyay and D. A. Lidar, Phys. Rev. A **72**, 042339 (2005); R. Chaves and L. Davidovich, Phys. Rev. A **82**, 052308 (2010); L. Aolita *et al.*, Phys. Rev. A **82**, 032317 (2010).

[9] A. R. R. Carvalho, F. Mintert, and A. Buchleitner, Phys. Rev. Lett. **93**, 230501 (2004).

[10] F. Lastra, G. Romero, C. E. Lopez, M. França Santos and J. C. Retamal, Phys. Rev A **75**, 062324 (2007).

[11] O. Gühne, F. Bodoky, and M. Blaauboer, Phys. Rev. A **78**, 060301(R) (2008).

[12] C. E. López, G. Romero, F. Lastra, E. Solano, and J. C. Retamal, Phys. Rev. Lett. **101**, 080503 (2008).

[13] A. R. P. Rau, M. Ali and G. Alber, EPL **82**, 40002 (2008); M. Ali, G. Alber, and A. R. P. Rau, J. Phys. B: At. Mol. Opt. Phys. **42**, 025501 (2009); M. Ali, J. Phys. B: At. Mol. Opt. Phys. **43**, 045504 (2010); M. Ali, Phys. Rev. A **81**, 042303 (2010).

[14] Y.S. Weinstein *et al.*, Phys. Rev. A **85**, 032324 (2012); S. N. Filippov, A. A. Melnikov, and M. Ziman, Phys. Rev. A **88**, 062328 (2013).

[15] M. Ali and O. Gühne, J. Phys. B: At. Mol. Opt. Phys. **47**, 055503 (2014).

[16] B. Jungnitsch, T. Moroder, and O. Gühne, Phys. Rev. Lett. **106**, 190502 (2011); L. Novo, T. Moroder, and O. Gühne, Phys. Rev. A **88**, 012305 (2013); M. Hofmann, T. Moroder, and O. Gühne, J. Phys. A: Math. Theor. **47**, 155301 (2014).

[17] S. Daffer, K. Wodkiewicz, J. D. Cresser, and J. K. McIver, Phys. Rev. A **70**, 010304 (2004).

[18] J. P. G. Pinto, G. Karpat, and F. F. Fanchini, Phys. Rev. A **88**, 034304 (2013).

[19] A. Peres, Phys. Rev. Lett. **77**, 1413 (1996).

[20] L. Vandenberghe and S. Boyd, SIAM Rev. **38**, 49 (1996).

[21] J. Löfberg, YALMIP: A Toolbox for Modeling and Optimization in MATLAB. Proceedings of the CACSD Conference, Taipei, Taiwan (2004).

[22] Program `PPTmixer`, weblink at `mathworks.com/matlabcentral/fileexchange/30968`.

[23] G. Vidal and R.F. Werner, Phys. Rev. A **65** 032314 (2002).

[24] B. Jungnitsch, T. Moroder, and O. Gühne, Phys. Rev. A **84**, 032310 (2011).

[25] G. Tóth, Comput. Phys. Comm. **179**, 430 (2008).

[26] L. Hartmann *et al.*, J. Phys. B: At. Mol. Opt. Phys **40** S1 (2007).

[27] M. Hein *et al.*, quant-ph/0602096.

[28] C. Kruszynska and B. Kraus, Phys. Rev. A **79**, 052304 (2009).

[29] A. Borras, A. P. Majtey, A. R. Plastino, M. Casas, and A. Plastino, Phys. Rev. A **79**, 022108 (2009).

[30] J. Novotný, G. Alber, and I. Jex, Phys. Rev. Lett. **107**, 090501 (2011).

[31] O. Gühne and M. Seevinck, N. J. Phys. **12**, 053002 (2010).

[32] S. N. Filippov, T. Rybár, and M. Ziman, Phys. Rev. A **85**, 012303 (2012).